

AD

TECHNICAL REPORT ARCCB-TR-97002

**ELECTRON TRANSPORT IN HIGHLY
TEXTURED METAL FILMS GROWN BY
PARTIALLY IONIZED BEAM DEPOSITION**

**S. R. SOSS
B. GITTLEMAN
K. E. MELLO
T.-M. LU
S. L. LEE**

JANUARY 1997



**US ARMY ARMAMENT RESEARCH,
DEVELOPMENT AND ENGINEERING CENTER
CLOSE COMBAT ARMAMENTS CENTER
BENÉT LABORATORIES
WATERVLIET, N.Y. 12189-4050**



APPROVED FOR PUBLIC RELEASE; DISTRIBUTION UNLIMITED

19970408 011

DTIC QUALITY INSPECTED 3

DISCLAIMER

The findings in this report are not to be construed as an official Department of the Army position unless so designated by other authorized documents.

The use of trade name(s) and/or manufacturer(s) does not constitute an official indorsement or approval.

DESTRUCTION NOTICE

For classified documents, follow the procedures in DoD 5200.22-M, Industrial Security Manual, Section II-19 or DoD 5200.1-R, Information Security Program Regulation, Chapter IX.

For unclassified, limited documents, destroy by any method that will prevent disclosure of contents or reconstruction of the document.

For unclassified, unlimited documents, destroy when the report is no longer needed. Do not return it to the originator.

REPORT DOCUMENTATION PAGE

Form Approved
OMB No. 0704-0188

Public reporting burden for this collection of information is estimated to average 1 hour per response, including the time for reviewing instructions, searching existing data sources, gathering and maintaining the data needed, and completing and reviewing the collection of information. Send comments regarding this burden estimate or any other aspect of this collection of information, including suggestions for reducing this burden, to Washington Headquarters Services, Directorate for Information Operations and Reports, 1215 Jefferson Davis Highway, Suite 1204, Arlington, VA 22202-4302, and to the Office of Management and Budget, Paperwork Reduction Project (0704-0188), Washington, DC 20503.

1. AGENCY USE ONLY (Leave blank)	2. REPORT DATE January 1997	3. REPORT TYPE AND DATES COVERED Final	
4. TITLE AND SUBTITLE ELECTRON TRANSPORT IN HIGHLY TEXTURED METAL FILMS GROWN BY PARTIALLY IONIZED BEAM DEPOSITION		5. FUNDING NUMBERS AMCMS No. 6111.01.91A1.1	
6. AUTHOR(S) S.R. Soss (RPI, Troy, NY), B. Gittleman (RPI), K.E. Mello (RPI), T.-M. Lu (RPI), and S.L. Lee			
7. PERFORMING ORGANIZATION NAME(S) AND ADDRESS(ES) U.S. Army ARDEC Benet Laboratories, AMSTA-AR-CCB-O Watervliet, NY 12189-4050		8. PERFORMING ORGANIZATION REPORT NUMBER ARCCB-TR-97002	
9. SPONSORING / MONITORING AGENCY NAME(S) AND ADDRESS(ES) U.S. Army ARDEC Close Combat Armaments Center Picatinny Arsenal, NJ 07806-5000		10. SPONSORING / MONITORING AGENCY REPORT NUMBER	
11. SUPPLEMENTARY NOTES Presented at the Materials Research Society Fall Conference, Boston, MA, 26 November - 1 December 1995. Published in proceedings of the conference.			
12a. DISTRIBUTION / AVAILABILITY STATEMENT Approved for public release; distribution unlimited.		12b. DISTRIBUTION CODE	
13. ABSTRACT (Maximum 200 words) In principle, the resistivity of bulk face-centered-cubic (fcc) materials should not depend on the orientation due to the fact that the conductivity tensor is single valued. However, we show that this conclusion is not valid for thin films. Deposition of highly oriented aluminum, silver, and copper films on amorphous substrates using the partially ionized beam (PIB) technique exhibits a resistivity that is strongly correlated with the texture, i.e., the tighter the texture, the lower the film resistivity. We model the film as an array of grains whose grain boundaries can be considered as delta function potentials for electron scattering, and the strength of the potentials can be calculated from the measured resistivity of the films. On the other hand, the fiber texture distribution of the films is obtained from X-ray pole figure measurements, and Monte-Carlo simulations are then performed using these data to determine the average dislocation density at the grain boundaries due to the grain-to-grain crystallographic mismatch. We show that the transmittance coefficient for electron scattering, and therefore, the film resistivity, is a monotonically increasing function of the average dislocation density. We, therefore, conclude that the structure of grain boundaries in a thin film provides the necessary mechanism by which the resistivity of an fcc cubic metal can depend on the texture.			
14. SUBJECT TERMS Partially Ionized Beam Deposition, Aluminum Films, Silver Films, Copper Films, Resistivity, Monte-Carlo Simulation, Electron Transport		15. NUMBER OF PAGES 11	
		16. PRICE CODE	
17. SECURITY CLASSIFICATION OF REPORT UNCLASSIFIED	18. SECURITY CLASSIFICATION OF THIS PAGE UNCLASSIFIED	19. SECURITY CLASSIFICATION OF ABSTRACT UNCLASSIFIED	20. LIMITATION OF ABSTRACT UL

TABLE OF CONTENTS

	Page
ACKNOWLEDGEMENTS	ii
INTRODUCTION	1
EXPERIMENTAL PROCEDURE	2
RESULTS	3
SIMULATION	4
CONCLUSIONS	5
REFERENCES	6

TABLES

1. Volume Fraction Distribution for Selected Silver, Copper, and Aluminum Films 7

LIST OF ILLUSTRATIONS

1. Change in the resistivity with changing ion energy used during the deposition 9

ACKNOWLEDGEMENTS

This work was partially supported by the National Science Foundation, Grant Number NSF ECS-9310613.

INTRODUCTION

One of the first researchers to identify that resistivity could depend on the size of the sample was Fuchs (ref 1), whose work was later extended and corrected by Sondheimer (ref 2). Mayadas and Shatzkes extended the work of Fuchs-Sondheimer to include the surfaces at the grain boundary (ref 3). The Mayadas-Shatzkes model consists of an array of grains whose boundaries are perpendicular to the electron flow in the medium. Later, Tellier et al. were to extend the results of the Mayadas-Shatzkes model into three dimensions (refs 4,5). Due to the recent demands on interconnect technology, another look into resistivity mechanisms is warranted. With the increased control of film microstructure made possible by current deposition technology, it is necessary to explore the effects of microstructure on the resistivity.

In keeping with the models presented by Mayadas and Shatzkes as well as Tellier, the film is assumed to be composed of grains that are cube-like in nature. The cube length is assumed to coincide with the average grain size in the film. In this manner, the grain size is not limited to that of the film thickness, but can instead be treated quite independently.

In the case of a film with grains, the mean free path is due to the interactions of the electrons with lattice distortions, as well as the interactions with the grain boundaries. The simplest form for this effective mean free path is to assume that the two are independent scattering mechanisms. This is certainly not correct, however deviations from this rule are not expected to be large. The mean free path due to grain boundaries alone is given by (refs 4,5)

$$\lambda_g = \frac{d}{\log(1/t)\{C^2 + (1 - C)|\cos\theta|\}} \quad (1)$$

where t is the probability of an electron to be specularly transmitted through the grain boundary, d is the average grain size in the film, and $\{\theta, \phi\}$ represent the trajectory of the electron. Equation (1) is obtained by the approximation that $C = |\cos \phi| + |\sin \phi| \approx 4/\pi$. If λ_0 is the single-crystalline mean free path, then the mean free path for the film is given by Matthiessen's rule, $1/\lambda = 1/\lambda_0 + 1/\lambda_g$.

If the film thickness is given by a , the probability for specular reflection of an electron that interacts with the film interface is given by p , and recalling that $\lambda = \bar{v}\tau$ when solving the Boltzmann equation, we obtain

$$\begin{aligned}
\sigma = \sigma_0 & \left\{ \frac{3}{2} \int_0^{\pi/2} \left[1 + \frac{\lambda_0}{\lambda_g(\theta)} \right]^{-1} \sin^3 \theta d\theta \right. \\
& - \frac{3\lambda_0}{4a} \int_0^{\pi/2} \left[1 + \frac{\lambda_0}{\lambda_g(\theta)} \right]^{-1} \cos \theta \sin^3 \theta \frac{1-p}{1-p \exp\left(-\frac{a}{\lambda_0 \cos \theta} \left[1 + \frac{\lambda_0}{\lambda_g(\theta)} \right] \right)} \\
& \left. \times \left[1 - \exp\left(-\frac{a}{\lambda_0 \cos \theta} \left[1 + \frac{\lambda_0}{\lambda_g(\theta)} \right] \right) \right] d\theta \right\} \quad (2)
\end{aligned}$$

where λ_g is left inside the θ -integration due to its dependence on the electron trajectory as given by equation (1). Of course, the resistivity for the film is again given simply as $\rho = 1/\sigma$.

As can be seen from equation (2), there are now four major parameters for the determination of the thin film resistivity. These are:

- The ratios between the bulk mean free path and the film thickness, λ_0/a
- The ratio between the bulk mean free path and the grain size that enters through λ_g , λ_0/d
- The probability for specular reflectance at the film surfaces, p
- The transmittance probability through a grain boundary, t

This report will be concerned with the last parameter, t . Because the transmittance through the grain boundary can be influenced by the nature of the boundary itself, it should not be surprising if texture can play a role in varying this parameter.

EXPERIMENTAL PROCEDURE

The partially ionized beam (PIB) deposition technique (ref 6) was used to deposit the films for this work. The benefits of using the PIB over other deposition techniques is that the grain orientation distribution can be changed while keeping the grain size relatively constant. The PIB technique achieves this through the use of ion assist. However, unlike sputtering, the ions used are derived from the neutral vapor stream. Thus, they are incorporated in the film as host material rather than as an impurity. The percentage on ions striking the film surface in this fashion can be varied between 0.1 and 5 percent of the neutral flux, and the energy of the incident ions can be varied between 0 and 3.5 keV. In our study, the glass substrates were held at room

temperature during the deposition, which occurred at a work vacuum between 5×10^{-5} Pa and 3×10^{-4} Pa. A metal clip was attached to the surface of the glass to prevent charging of the surface during depositions and to avoid pinholing in the films (ref 7). A base vacuum of better than 5×10^{-5} Pa was achieved prior to deposition. Silver was typically deposited with a deposition rate of about 10 to 15 Å/s. Copper was deposited under similar conditions with a rate of approximately 14 Å/s. The deposition rate for aluminum was held lower at approximately 5 Å/s. All films were approximately 1500 to 2000 Å thick.

The film thickness was monitored during deposition using a quartz crystal monitor and confirmed using a Tencor Alpha Step profilometer. Sheet resistance was measured for the films using a standard in-line four-point probe. Measurement of the grain size was determined by both X-ray and Atomic Force Microscopy (AFM) techniques. Conventional Bragg 2θ measurements were performed to obtain qualitative information as to the grain orientations with respect to the substrate surface. Pole figure analysis and its subset, the fiber texture plot, were used to determine the volume fraction information as well as angular distributions of the grains in the film. Measurements were performed using a Scintag 2000 X-ray diffractometer.

RESULTS

Changing the energy of the ions during the deposition of silver, copper, and aluminum resulted in a change in the resistivity of the as-deposited film. In all cases there was a clear minimum in the measured resistivity with ion energy. The changes observed were too great to be attributed to impurity effects. Regardless of the ion energy used during deposition, the grain size was relatively constant. The grain distributions in all of the films were seen to be monomodal.

The predicted resistivity was calculated using equation (2). We have used the values for the transmittance probability commonly found in the literature, as well as the measured grain sizes in the film. As there are no listed transmittance values for silver, the copper value was used instead. The open triangles in Figure 1 show the calculated resistivity for silver, copper, and aluminum. Fiber texture and pole scans were taken for each volume component using Schultz geometry. Table 1 summarizes the results of the fiber texture measurements. Aluminum can be seen to exhibit a trend in the resistivity with the $\langle 111 \rangle$ volume fraction. The lack of a $\langle 200 \rangle$ volume fraction indicates that it is of higher probability that two grains neighboring each other will be of the same orientation, i.e., of $\langle 111 \rangle$ type. If this is the case, then an electron that travels from one grain to its neighbor is less likely to see a large lattice change, and hence, experience a higher probability of specular transmittance. In this manner, the resistivity would not be controlled by any other volume fraction, but rather by the degree of lattice change between neighboring grains.

SIMULATION

Monte-Carlo methods were used to determine the average effective grain boundary dislocation density for each film. From the measured fiber texture information, the volume fractions as well as the Gaussian distributions of the grains within the volume fraction are known. Also from this information, a film is generated where each successive grain is created such that the grain type follows the probabilities of the volume fractions. In addition, the tilt angle for the grain is then given by the measured Gaussian distribution (except for the random grains, which are given a flat distribution). The azimuthal rotations of the grains are determined randomly to coincide with the observed fiber texture of the films.

From the knowledge of each grain orientation, the atomic positions at the grain boundary interface can be determined. The areal density of atoms at the boundary from atoms on either side is then compared. The dislocation density is obtained by looking at the degree of area difference that exists in the change from one lattice orientation to the other. The difference in this area represents those atoms that are not accommodated by the switch in lattice orientations, and so are due to dislocations. From the knowledge of the size of the Burgers vector in the material, the dislocation density at the grain boundary can be determined. At high tilt angles, the dislocations in a real crystal will begin to coalesce into super-dislocations and eventually void formation at the boundary will occur. In fact, the concept of a dislocation density in this case is likely to have little physical meaning. However, the values given by the simulation should still serve as a valid tracking number, albeit a physically meaningless one. The values of the dislocation density, ρ_{dd} , should be used solely for their trend indications, and the absolute values should not be taken too precisely.

Stripes of 1000 grains or more were simulated and averaged over more than 100 runs. It can be seen that the minimum in resistivity follows with the dislocation density at the grain boundary when plotted as a function of the ion energy used during deposition. Figure 1 shows a representation of this correlation for the copper, silver, and aluminum films. It seems apparent that while grain size and impurity concentration cannot account for the variation in the resistivity, perhaps the grain boundary dislocation density can.

In order to return to the original problem of the specular transmittance parameter, t , for an electron to pass through the grain boundary, it is necessary to determine how the transmittance and the dislocation density are related. A simple model can be used whereby the transmittance should linearly decrease with increasing dislocation density.

Using the measured resistivities and the grain size as measured from AFM, the transmittance coefficient in the Tellier model can be calculated for each film. The specular transmittance probabilities obtained from the resistivity values are then plotted against the simulated results for the effective grain boundary dislocation densities. The results for silver, aluminum, and copper are that the specular transmittance probability always decreases linearly

with the effective dislocation density. The minimum points in the resistivity curves of Figure 1 correspond to the lowest effective dislocation density, and consequently the highest electron transmission probability. With silver, for example, at the minimum resistivity we obtain a transmission coefficient of 0.9.

CONCLUSIONS

The resistivity of a thin metal film has been shown to depend not only on the grain size and impurity concentration, but also on the degree of texture. Texture plays a role in the resistivity as a second-order effect, however it can be seen to dramatically affect the resistivity when other parameters are held constant.

Using the PIB deposition system, thin silver, copper, and aluminum films were grown with varying degrees of texture while keeping the grain size relatively constant. A Monte-Carlo simulation was developed to determine the effective dislocation density at the grain boundary for a given film. Using the measured texture distribution from X-ray pole figure techniques, the calculated dislocation density was seen to track well with the measured resistivity. A simple model was proposed that the probability for specular transmittance of a conduction electron at the grain boundary decreases with increasing dislocation density.

REFERENCES

1. K. Fuchs, *Proceedings of the Cambridge Philosophical Society*, Vol. 34, 1938, p. 100.
2. E.H. Sondheimer, *Advances in Physics*, Vol. 1 No. 1, 1952, p. 1.
3. A.F. Mayadas and M. Shatzkes, "Electrical-Resistivity Model for Polycrystalline Films: The Case of Arbitrary Reflection at External Surfaces," *Physical Review B*, Vol. 1, No. 4, February 1970, p. 1382.
4. C.R. Tellier, C.R. Pichard, and A.J. Tosser, "Statistical Model of Electrical Conduction in Polycrystalline Metals," *Thin Solid Films*, Vol. 61, February 1979, p. 349.
5. C.R. Pichard, C.R. Tellier, and A.J. Tosser, "A Three-Dimensional Model for Grain Boundary Resistivity in Metal Films," *Thin Solid Films*, Vol. 62, March 1979, p. 189.
6. S.-N. Mei and T.-M. Lu, *Journal of Vacuum Science and Technology A*, Vol. 6, 1988, p. 9.
7. S.R. Soss, C.A. Cook, and T.-M. Lu, "Partially Ionized Beam Deposition of Ag Films on Insulating Substrates," *Journal of Applied Physics*, Vol. 77, No. 6, March 1995, p. 2735.
8. P. Bai, "Effects of Low Energy Ion Bombardment on the Growth of Cu Films," PhD Thesis, Rensselaer Polytechnic Institute, Troy, NY, February 1991.
9. B.D. Gittleman, "The Effects of Low Energy Ion Bombardment on the Growth of Thin Films: Model and Experiment," PhD Thesis, Rensselaer Polytechnic Institute, Troy, NY, February 1995.
10. A.S. Yapsir, "Ion Implantation Effects on the Metal-Semiconductor Interfaces," PhD Thesis, Rensselaer Polytechnic Institute, Troy, NY, December 1988.

Table 1. Volume Fraction Distribution for Selected Silver, Copper, and Aluminum Films

Ion Energy (eV)	<111> Fraction				<200> Fraction				Random Vol. Frac.
	Vol. Frac.	A	σ	ω_{90}	Vol. Frac.	A	σ	ω_{90}	
Silver:									
860	0.513	15.161	8.859	16.75	0.194	1.502	15.764	21.50	0.297
1030	0.550	18.730	7.449	16.50	0.196	1.793	14.713	21.50	0.255
1180	0.546	18.768	7.597	15.50	0.173	1.506	15.404	21.00	0.281
1380	0.471	15.328	8.709	17.00	0.182	1.752	13.813	20.00	0.347
1550	0.512	16.927	8.198	16.375	0.182	1.554	13.602	21.25	0.306
1720	0.568	17.806	8.557	16.00	0.202	1.638	15.764	21.50	0.281
1890	0.466	15.058	8.798	17.00	0.186	1.646	15.314	20.75	0.349
Copper:									
870	0.528	16.377	6.996	18.75	0.251	1.709	19.068	23.25	0.141
1040	0.573	16.873	7.656	16.25	0.385	4.122	14.713	20.75	0.043
1190	0.448	21.082	6.907	15.00	0.231	2.492	13.213	17.75	0.276
1380	0.578	21.068	6.756	15.25	0.295	2.495	16.816	20.00	0.053
1550	0.674	24.583	6.396	16.50	0.306	2.572	17.566	22.00	0.020
1720	0.479	18.100	7.357	16.00	0.360	2.410	17.716	24.00	0.135
1890	0.641	19.936	6.996	15.50	0.332	2.170	18.617	23.75	0.026

Aluminum:												
740	0.320	13.225	9.158	18.50	0.214	1.556	15.615	22.75	0.465			
910	0.304	11.096	9.158	20.00	0.245	1.739	14.713	24.25	0.451			
1080	0.881	23.925	7.356	16.00	--	--	--	--	0.119			
1250	0.462	6.695	9.401	18.25	0.108	0.677	19.518	22.25	0.430			
1420	0.439	14.359	10.059	17.75	0.204	1.582	16.966	23.25	0.330			

Note: A is the Gaussian peak height, 68 percent of the values are in 1σ , and ω_{90} is the angle at which 90 percent of the integrated intensity is included.

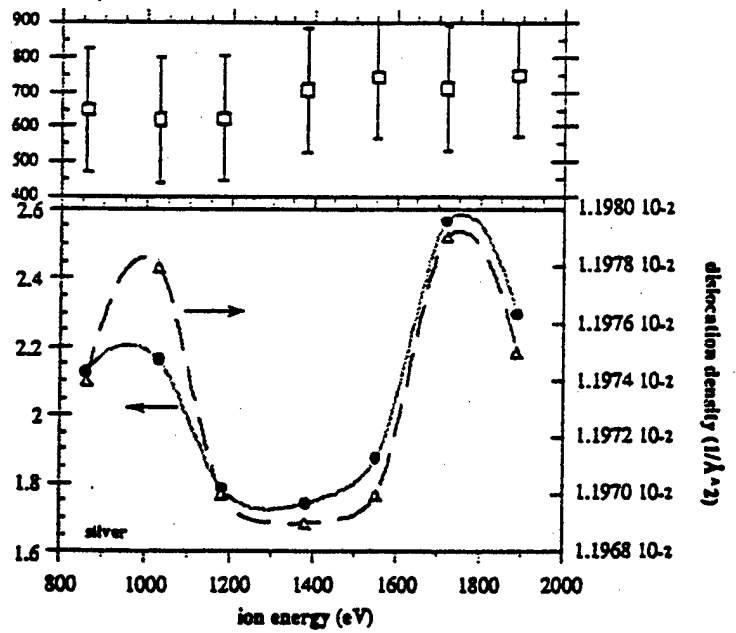
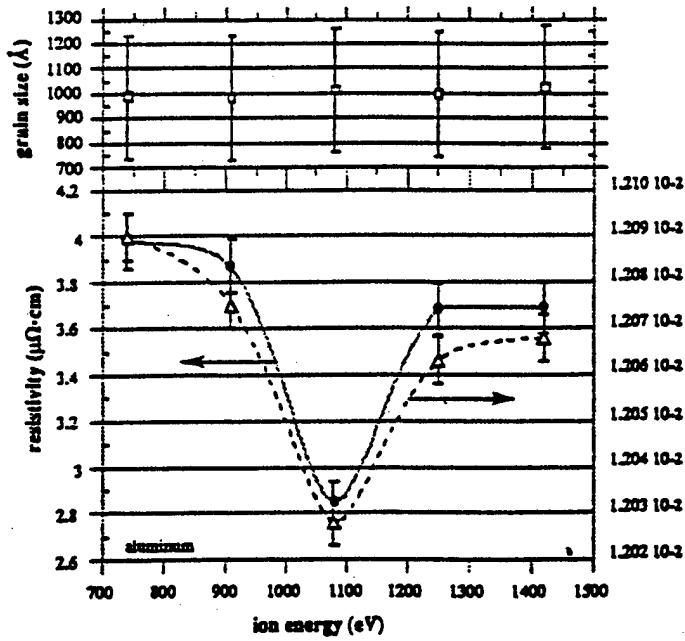
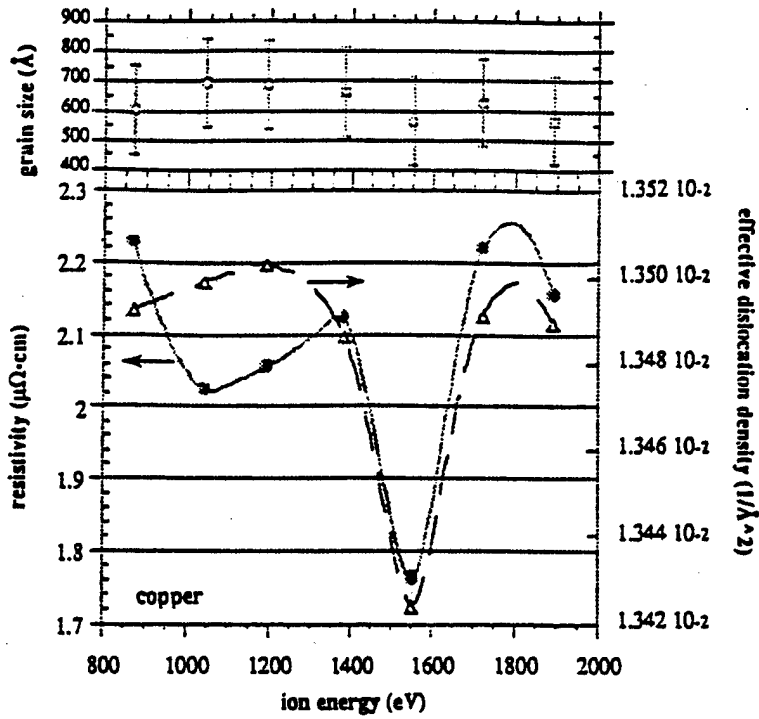


Figure 1. Change in the resistivity with changing ion energy used during the deposition. The solid circles represent the measured resistivity. The open triangles are predicted values using the Fuchs-Sondheimer/Tellier model for resistivity. The simulated dislocation densities are also plotted.

TECHNICAL REPORT INTERNAL DISTRIBUTION LIST

	<u>NO. OF COPIES</u>
CHIEF, DEVELOPMENT ENGINEERING DIVISION	
ATTN: AMSTA-AR-CCB-DA	1
-DB	1
-DC	1
-DD	1
-DE	1
 CHIEF, ENGINEERING DIVISION	
ATTN: AMSTA-AR-CCB-E	1
-EA	1
-EB	1
-EC	1
 CHIEF, TECHNOLOGY DIVISION	
ATTN: AMSTA-AR-CCB-T	2
-TA	1
-TB	1
-TC	1
 TECHNICAL LIBRARY	
ATTN: AMSTA-AR-CCB-O	5
 TECHNICAL PUBLICATIONS & EDITING SECTION	
ATTN: AMSTA-AR-CCB-O	3
 OPERATIONS DIRECTORATE	
ATTN: SIOVV-ODP-P	1
 DIRECTOR, PROCUREMENT & CONTRACTING DIRECTORATE	
ATTN: SIOVV-PP	1
 DIRECTOR, PRODUCT ASSURANCE & TEST DIRECTORATE	
ATTN: SIOVV-QA	1

NOTE: PLEASE NOTIFY DIRECTOR, BENÉT LABORATORIES, ATTN: AMSTA-AR-CCB-O OF ADDRESS CHANGES.

TECHNICAL REPORT EXTERNAL DISTRIBUTION LIST

	<u>NO. OF COPIES</u>		<u>NO. OF COPIES</u>
ASST SEC OF THE ARMY RESEARCH AND DEVELOPMENT ATTN: DEPT FOR SCI AND TECH THE PENTAGON WASHINGTON, D.C. 20310-0103	1	COMMANDER ROCK ISLAND ARSENAL ATTN: SMCRI-SEM ROCK ISLAND, IL 61299-5001	1
DEFENSE TECHNICAL INFO CENTER ATTN: DTIC-OCP (ACQUISITIONS) 8725 JOHN J. KINGMAN ROAD STE 0944 FT. BELVOIR, VA 22060-6218	2	MIAC/CINDAS PURDUE UNIVERSITY 2595 YEAGER ROAD WEST LAFAYETTE, IN 47906-1398	1
COMMANDER U.S. ARMY ARDEC ATTN: AMSTA-AR-AEE, BLDG. 3022 AMSTA-AR-AES, BLDG. 321 AMSTA-AR-AET-O, BLDG. 183 AMSTA-AR-FSA, BLDG. 354 AMSTA-AR-FSM-E AMSTA-AR-FSS-D, BLDG. 94 AMSTA-AR-IMC, BLDG. 59 PICATINNY ARSENAL, NJ 07806-5000	1 1 1 1 1 1 2	COMMANDER U.S. ARMY TANK-AUTMV R&D COMMAND ATTN: AMSTA-DDL (TECH LIBRARY) WARREN, MI 48397-5000	1
DIRECTOR U.S. ARMY RESEARCH LABORATORY ATTN: AMSRL-DD-T, BLDG. 305 ABERDEEN PROVING GROUND, MD 21005-5066	1	COMMANDER U.S. MILITARY ACADEMY ATTN: DEPARTMENT OF MECHANICS WEST POINT, NY 10966-1792	1
DIRECTOR U.S. ARMY RESEARCH LABORATORY ATTN: AMSRL-WT-PD (DR. B. BURNS) ABERDEEN PROVING GROUND, MD 21005-5066	1	U.S. ARMY MISSILE COMMAND REDSTONE SCIENTIFIC INFO CENTER ATTN: AMSMI-RD-CS-R/DOCUMENTS BLDG. 4484 REDSTONE ARSENAL, AL 35898-5241	2
DIRECTOR U.S. MATERIEL SYSTEMS ANALYSIS ACTV ATTN: AMXSY-MP ABERDEEN PROVING GROUND, MD 21005-5071	1	COMMANDER U.S. ARMY FOREIGN SCI & TECH CENTER ATTN: DRXST-SD 220 7TH STREET, N.E. CHARLOTTESVILLE, VA 22901	1
		COMMANDER U.S. ARMY LABCOM, ISA ATTN: SLCIS-IM-TL 2800 POWER MILL ROAD ADELPHI, MD 20783-1145	1

NOTE: PLEASE NOTIFY COMMANDER, ARMAMENT RESEARCH, DEVELOPMENT, AND ENGINEERING CENTER,
BENÉT LABORATORIES, CCAC, U.S. ARMY TANK-AUTOMOTIVE AND ARMAMENTS COMMAND,
AMSTA-AR-CCB-O, WATERVLIET, NY 12189-4050 OF ADDRESS CHANGES.

TECHNICAL REPORT EXTERNAL DISTRIBUTION LIST (CONT'D)

	<u>NO. OF COPIES</u>		<u>NO. OF COPIES</u>
COMMANDER U.S. ARMY RESEARCH OFFICE ATTN: CHIEF, IPO P.O. BOX 12211 RESEARCH TRIANGLE PARK, NC 27709-2211	1	WRIGHT LABORATORY ARMAMENT DIRECTORATE ATTN: WL/MNM EGLIN AFB, FL 32542-6810	1
DIRECTOR U.S. NAVAL RESEARCH LABORATORY ATTN: MATERIALS SCI & TECH DIV WASHINGTON, D.C. 20375	1	WRIGHT LABORATORY ARMAMENT DIRECTORATE ATTN: WL/MNMF EGLIN AFB, FL 32542-6810	1

NOTE: PLEASE NOTIFY COMMANDER, ARMAMENT RESEARCH, DEVELOPMENT, AND ENGINEERING CENTER,
BENÉT LABORATORIES, CCAC, U.S. ARMY TANK-AUTOMOTIVE AND ARMAMENTS COMMAND,
AMSTA-AR-CCB-O, WATERVLIET, NY 12189-4050 OF ADDRESS CHANGES.
